Global emission estimates and radiative impact of C_4F_{10}, C_5F_{12}, C_6F_{14}, C_7F_{16} and C_8F_{18}*

Diane J. Ivy, Matthew Rigby, Munkhbayar Baasandorj, James B. Burkholder and Ronald G. Prinn

MIT JOINT PROGRAM ON THE SCIENCE AND POLICY of GLOBAL CHANGE

*Reprinted from
Atmospheric Chemistry and Physics, 12: 7635–7645

Reprint 2012-37

The MIT Joint Program on the Science and Policy of Global Change combines cutting-edge scientific research with independent policy analysis to provide a solid foundation for the public and private decisions needed to mitigate and adapt to unavoidable global environmental changes. Being data-driven, the Program uses extensive Earth system and economic data and models to produce quantitative analysis and predictions of the risks of climate change and the challenges of limiting human influence on the environment—essential knowledge for the international dialogue toward a global response to climate change.

To this end, the Program brings together an interdisciplinary group from two established MIT research centers: the Center for Global Change Science (CGCS) and the Center for Energy and Environmental Policy Research (CEEPR). These two centers—along with collaborators from the Marine Biology Laboratory (MBL) at Woods Hole and short- and long-term visitors—provide the united vision needed to solve global challenges.

At the heart of much of the Program's work lies MIT's Integrated Global System Model. Through this integrated model, the Program seeks to: discover new interactions among natural and human climate system components; objectively assess uncertainty in economic and climate projections; critically and quantitatively analyze environmental management and policy proposals; understand complex connections among the many forces that will shape our future; and improve methods to model, monitor and verify greenhouse gas emissions and climatic impacts.

This reprint is one of a series intended to communicate research results and improve public understanding of global environment and energy challenges, thereby contributing to informed debate about climate change and the economic and social implications of policy alternatives.

Ronald G. Prinn and John M. Reilly,
Program Co-Directors

For more information, contact the Program office:

MIT Joint Program on the Science and Policy of Global Change
Postal Address:
Massachusetts Institute of Technology
77 Massachusetts Avenue, E19-411
Cambridge, MA 02139 (USA)
Location:
Building E19, Room 411
400 Main Street, Cambridge
Access:
Tel: (617) 253-7492
Fax: (617) 253-9845
Email: ***globalchange@mit.edu***
Website: ***http://globalchange.mit.edu/***

Atmos. Chem. Phys., 12, 7635–7645, 2012
www.atmos-chem-phys.net/12/7635/2012/
doi:10.5194/acp-12-7635-2012

Atmospheric Chemistry and Physics

Global emission estimates and radiative impact of C_4F_{10}, C_5F_{12}, C_6F_{14}, C_7F_{16} and C_8F_{18}

D. J. Ivy[1], M. Rigby[1,*], M. Baasandorj[2,3], J. B. Burkholder[2], and R. G. Prinn[1]

[1]Center for Global Change Science, Massachusetts Institute of Technology, Cambridge, Massachusetts, USA
[2]Earth System Research Laboratory, National Oceanic and Atmospheric Administration, Boulder, Colorado, USA
[3]Cooperative Institute for Research in Environmental Studies, University of Colorado, Boulder, Colorado, USA
[*]now at: Atmospheric Chemistry Research Group, University of Bristol, Bristol, UK

Correspondence to: D. J. Ivy (divy@mit.edu)

Received: 25 April 2012 – Published in Atmos. Chem. Phys. Discuss.: 24 May 2012
Revised: 13 August 2012 – Accepted: 15 August 2012 – Published: 22 August 2012

Abstract. Global emission estimates based on new atmospheric observations are presented for the acylic high molecular weight perfluorocarbons (PFCs): decafluorobutane (C_4F_{10}), dodecafluoropentane (C_5F_{12}), tetradecafluorohexane (C_6F_{14}), hexadecafluoroheptane (C_7F_{16}) and octadecafluorooctane (C_8F_{18}). Emissions are estimated using a 3-dimensional chemical transport model and an inverse method that includes a growth constraint on emissions. The observations used in the inversion are based on newly measured archived air samples that cover a 39-yr period, from 1973 to 2011, and include 36 Northern Hemispheric and 46 Southern Hemispheric samples. The derived emission estimates show that global emission rates were largest in the 1980s and 1990s for C_4F_{10} and C_5F_{12}, and in the 1990s for C_6F_{14}, C_7F_{16} and C_8F_{18}. After a subsequent decline, emissions have remained relatively stable, within 20 %, for the last 5 yr. Bottom-up emission estimates are available from the Emission Database for Global Atmospheric Research version 4.2 (EDGARv4.2) for C_4F_{10}, C_5F_{12}, C_6F_{14} and C_7F_{16}, and inventories of C_4F_{10}, C_5F_{12} and C_6F_{14} are reported to the United Nations' Framework Convention on Climate Change (UNFCCC) by Annex 1 countries that have ratified the Kyoto Protocol. The atmospheric measurement-based emission estimates are 20 times larger than EDGARv4.2 for C_4F_{10} and over three orders of magnitude larger for C_5F_{12} (with 2008 EDGARv4.2 estimates for C_5F_{12} at 9.6 kg yr^{-1}, as compared to 67±53 t yr^{-1} as derived in this study). The derived emission estimates for C_6F_{14} largely agree with the bottom-up estimates from EDGARv4.2. Moreover, the C_7F_{16} emission estimates are comparable to those of EDGARv4.2 at their peak in the 1990s, albeit significant underestimation for the other time periods. There are no bottom-up emission estimates for C_8F_{18}, thus the emission rates reported here are the first for C_8F_{18}. The reported inventories for C_4F_{10}, C_5F_{12} and C_6F_{14} to UNFCCC are five to ten times lower than those estimated in this study.

In addition, we present measured infrared absorption spectra for C_7F_{16} and C_8F_{18}, and estimate their radiative efficiencies and global warming potentials (GWPs). We find that C_8F_{18}'s radiative efficiency is similar to trifluoromethyl sulfur pentafluoride's (SF_5F_3) at 0.57 W m^{-2} ppb^{-1}, which is the highest radiative efficiency of any measured atmospheric species. Using the 100-yr time horizon GWPs, the total radiative impact of the high molecular weight perfluorocarbons emissions are also estimated; we find the high molecular weight PFCs peak contribution was in 1997 at 24 000 Gg of carbon dioxide (CO_2) equivalents and has decreased by a factor of three to 7300 Gg of CO_2 equivalents in 2010. This 2010 cumulative emission rate for the high molecular weight PFCs is comparable to: 0.02 % of the total CO_2 emissions, 0.81 % of the total hydrofluorocarbon emissions, or 1.07 % of the total chlorofluorocarbon emissions projected for 2010 (Velders et al., 2009). In terms of the total PFC emission budget, including the lower molecular weight PFCs, the high molecular weight PFCs peak contribution was also in 1997 at 15.4 % and was 6 % of the total PFC emissions in CO_2 equivalents in 2009.

Published by Copernicus Publications on behalf of the European Geosciences Union.

Table 1. Lifetimes, radiative efficiencies and global warming potentials (by mass) of C_4F_{10}, C_5F_{12}, C_6F_{14}, C_7F_{16} and C_8F_{18}.

Species	Lifetime [yr]	Radiative efficiencies [$W\,m^{-2}\,ppb^{-1}$]	Global warming potentials (GWPs) 20-yr horizon	100-yr horizon	500-yr horizon	Reference
C_4F_{10}	2600	0.33	6330	8860	12 500	Forster et al. (2007)
C_5F_{12}	4100	0.41	6510	9160	13 300	Forster et al. (2007)
C_6F_{14}	3200	0.49	6600	9300	13 300	Forster et al. (2007)
C_7F_{16}	(3000)	0.48	5630	7930	11 300	This Study
	3000	0.45	–	–	–	Bravo et al. (2010)
C_8F_{18}	(3000)	0.57	5920	8340	11 880	This Study
	3000	0.50	5280	7390	10 500	Bravo et al. (2010)

1 Introduction

Perfluorocarbons (PFCs) are potent greenhouse gases due to their long lifetimes and strong absorption in the infrared atmospheric window region, resulting in global warming potentials (GWPs) on a 100-yr time horizon of three to four orders of magnitude higher than that of carbon dioxide (CO_2) (see Table 1) (Forster et al., 2007). Subsequently, PFCs are considered to have a nearly permanent effect on the Earth's radiative budget, when human time scales are considered. PFCs are included as one of the six classes of greenhouse gases under the Kyoto Protocol to the United Nations' Framework Convention on Climate Change (UNFCCC).

Atmospheric observations and global emission estimates based on atmospheric measurements are available for the lower molecular weight PFCs: tetrafluoromethane (CF_4), hexafluoroethane (C_2F_6), octafluoropropane (C_3F_8) and octafluorocyclobutane (c−C_4F_8) (Mühle et al., 2010; Oram et al., 2012). The lower molecular weight PFCs are primarily emitted from the production of aluminum and usage in the semiconductor industry. Efforts are being made by both industries to reduce these emissions (International Aluminium Institute, 2011; Semiconductor Industry Association, 2001; World Semiconductor Council, 2005). Furthermore, CF_4 and C_2F_6 have a natural abundance due to a lithospheric source (Deeds et al., 2008; Harnisch et al., 1996a,b; Mühle et al., 2010). The global emission estimates by Mühle et al. (2010) and Oram et al. (2012) for the lower molecular weight PFCs concluded that bottom-up emission estimates, based on production information and end usage, were underestimated as compared to estimates constrained by atmospheric observations, particularly for C_3F_8 and c−C_4F_8. These studies illustrate the valuable constraint atmospheric observations provide in independently estimating emissions for the verification of bottom-up emission estimates.

Bottom-up emission estimates are provided by the Emission Database for Global Atmospheric Research version 4.2 (EDGARv4.2) for the high molecular weight PFCs: decafluorobutane (C_4F_{10}), dodecafluoropentane (C_5F_{12}), tetradecafluorohexane (C_6F_{14}) and hexadecafluoroheptane (C_7F_{16}) from 1970 to 2008 (ER-JRC/PBL, 2011). Furthermore, C_4F_{10}, C_5F_{12} and C_6F_{14} emissions are reported from 1990 to 2009 to UNFCCC by Annex 1 countries that have ratified the Kyoto Protocol (UNFCCC, 2011). However, no emission data are available for octadecafluorooctane (C_8F_{18}).

Since the early 1990s, these higher molecular weight PFCs have had a relatively minor role as replacements for ozone depleting substances (ODS), which are regulated under the Montreal Protocol (Harvey, 2000). Of which, the most significant emission source of the high molecular weight PFCs are from their use as solvents in electronics and precision cleaning, which was approved under the Significant New Alternatives Policy (SNAP) program (Air and Radiation Global Programs Division, 2006; Tsai, 2009). There are also small niche markets for C_4F_{10} and C_6F_{14} as fire suppressants (Forte, Jr. et al., 2003; Kopylov, 2002; Tsai, 2009) and C_4F_{10}, C_5F_{12} and C_6F_{14} as refrigerants (ER-JRC/PBL, 2011; Schwaab et al., 2005; Tsai, 2009). Because of the PFCs' large GWPs, emissions of these high molecular weight PFCs as ODS replacements are expected to be decreasing as they are being replaced with lower GWP alternatives (Harvey, 2000; United Nations Environment Programme, 1999).

The PFCs, which are liquid at room temperature, C_5F_{12}-C_8F_{18} are additionally being used in the semiconductor manufacturing industry as heat transfer fluids and in vapor phase reflow soldering (3M Electronics Markets Materials Division, 2003; Tsai, 2009; Tuma and Tousignant, 2001). This emission source is a first-of-a-kind for fluorinated compounds (Tuma and Tousignant, 2001). While the semiconductor industry is making efforts to reduce PFC emissions, their efforts are focused on reducing emissions of the lower molecular weight PFCs. Therefore emission estimates based on atmospheric observations of the high molecular weight PFCs are valuable for determining if these industries are indeed reducing all PFC emissions.

Laube et al. (2012) provided global emission estimates using a 2-dimensional model and atmospheric observations for C_4F_{10}, C_5F_{12}, C_6F_{14} and C_7F_{16}. However, the emission estimates by Laube et al. (2012) were determined qualitatively and not constrained by an inverse method, and therefore

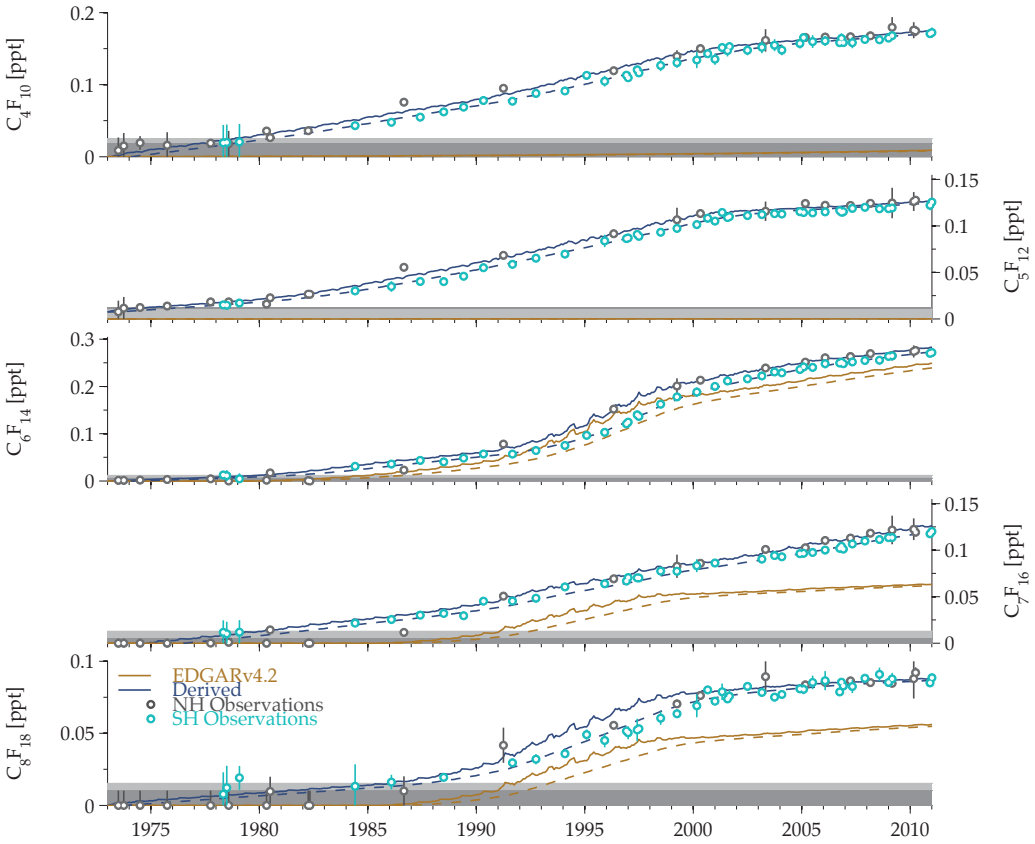

Fig. 1. MOZARTv4.5 model output at the observation grid cells (Northern Hemisphere – solid line and Southern Hemisphere – dashed line) for the reference run using emissions based on EDGARv4.2 (yellow lines) and the final derived emissions (blue lines). The open circles are the atmospheric observations (Northern Hemisphere – grey and Southern Hemisphere – light blue), with the vertical lines being the associated observational uncertainty. The detection limits for the instruments are shown as the grey shading, with dark grey for the SIO instrument and the light grey for the CSIRO instrument.

their emissions were not optimally determined. In this study, we present global annual emission estimates for the high molecular weight PFCs, C_4F_{10}, C_5F_{12}, C_6F_{14}, C_7F_{16} and C_8F_{18}, based on new atmospheric measurements presented in Ivy et al. (2012). Emissions are estimated using a 3-dimensional chemical transport model (CTM), the Model of Ozone and Related chemical Tracers (MOZARTv4.5), and an inverse method, in which the atmospheric observations and an independent estimate of the emission growth rates are used as constraints (Emmons et al., 2010; Rigby et al., 2011). The derived emissions based on atmospheric measurements are compared to the available bottom-up emission data from EDGARv4.2 and the inventories reported to UNFCCC. Furthermore, we present measured infrared (IR) absorption spectra for C_7F_{16} and C_8F_{18} in order to provide estimates of their GWPs. Thus, we provide an updated total of the radiative impact of global PFC emissions in CO_2 equivalents from 1978 to 2009, now including the high molecular weight PFCs.

2 Inverse modeling

2.1 Observations

The atmospheric observations of the high molecular weight PFCs used to constrain the derived emission estimates are based on archived air samples that were measured using the Advanced Global Atmospheric Gases Experiment (AGAGE) "Medusa" systems and cover a time period from 1973 to 2011, see Ivy et al. (2012) for details. The atmospheric histories of the high molecular weight PFCs, shown in Fig. 1, are based on measurements of 36 Northern Hemisphere (NH) archived air samples, filled primarily at Trinidad Head, California (41.05° N, 124.05° W), and 46 Southern Hemisphere (SH) archived air samples, filled at Cape Grim, Tasmania, Australia (40.68° S, 144.69° E). For this modeling study, the observations were assumed to be representative of the monthly mean hemispheric background tropospheric air. This is a valid assumption given that the archived air samples were filled under baseline conditions.

Associated with each observation is an estimate of its uncertainty, which includes the estimated uncertainties associated with the measurements, the sampling frequency, grid cell model-mismatch and use of repeated dynamics when applicable, see Eq. (1) (Rigby et al., 2010).

$$\sigma^2_{\text{observational}} = \sigma^2_{\text{measurement}} + \sigma^2_{\text{sampling frequency}} + \sigma^2_{\text{mismatch}} + \sigma^2_{\text{dynamics}} \quad (1)$$

The measurement uncertainty, $\sigma_{\text{measurement}}$, is the repeatability of each archived air sample measurement and is taken as the 1-σ standard deviation of the repeat sample measurements. The sampling frequency uncertainty, $\sigma_{\text{sampling frequency}}$, provides a measure of the uncertainty in our assumption that a single flask is representative of the monthly mean baseline variability. Since high frequency data are not available, the sampling frequency uncertainty was estimated as the standard deviation of daily modeled output from the CTM over one month at the observation grid cell. The model-mismatch error, σ_{mismatch}, is an estimate of the uncertainty in the assumption that the model grid cell is representative of a single point measurement. We estimated the model-mismatch error using the CTM as the 1-σ standard deviation of the surrounding eight grid cells and the grid cell that contains the observation location from the mean of all nine cells (Chen and Prinn, 2006). Reanalysis meteorological data are not available for years prior to 1990 for use in the CTM (i.e. ERA-40 data not are available for use in MOZARTv4.5); therefore, we used repeated meteorological data from 1990 for the years from 1971 to 1989 in the CTM and 2008 for the years from 2009 to 2011. In order to characterize the uncertainty in this use of repeated dynamics, σ_{dynamics}, a one year simulation was run multiple times with different meteorological data from other years, while the emissions and initial conditions were held constant (Rigby et al., 2010). This introduced a mean uncertainty of 5 % at the observation grid cells and was included in the observational uncertainty. Lastly, observations that were below the detection limit of the instruments were assigned a minimum uncertainty equal to that of the detection limit.

2.2 Bottom-up emission estimates

Bottom-up emission estimates are available from EDGARv4.2 (ER-JRC/PBL, 2011). EDGARv4.2 has global annual emission estimates by source for C_4F_{10}, C_5F_{12}, C_6F_{14} and C_7F_{16} from 1970 to 2008, see Fig. 2, and on a 0.1° longitude by 0.1° latitude gridded data, with non-zero emissions starting in 1971 for C_4F_{10}, 1986 for C_5F_{12}, 1980 for C_6F_{14} and 1986 for C_7F_{16}. There are no EDGARv4.2 estimates available for C_8F_{18}, therefore C_7F_{16} estimates were used as a proxy. This is under the assumption that as C_7F_{16} and C_8F_{18} have similar properties, they will most likely have similar emission sources. Furthermore, as the archived samples are assumed to be representative of well-mixed background hemispheric air in the regions

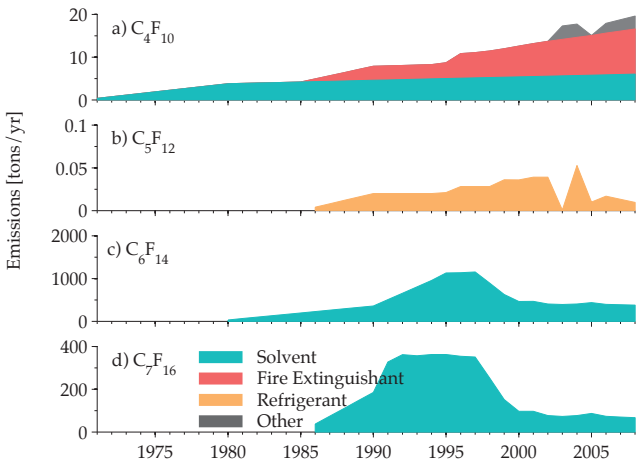

Fig. 2. Global annual bottom-up emission estimates from 1971 to 2008 by source from EDGARv4.2 for **(a)** C_4F_{10}, **(b)** C_5F_{12}, **(c)** C_6F_{14} and **(d)** C_7F_{16} (ER-JRC/PBL, 2011). (Note: C_8F_{18} is not available from EDGARv4.2.)

they were collected, the emission estimates should be relatively insensitive to the relative hemispheric spatial distributions of emissions. For 2009 to 2011, the emissions were linearly interpolated from the 2007 to 2008 data. The annual 0.1° longitude by 0.1° latitude emissions were regridded to a horizontal resolution of 2.8° longitude by 2.8° latitude for use in the CTM. Inventories for C_4F_{10}, C_5F_{12} and C_6F_{14} are also reported to UNFCCC by Annex 1 countries that have ratified the Kyoto Protocol. However as the reported inventories to UNFCCC are not global, we used the EDGARv4.2 data in the CTM to produce the reference runs and to estimate the sensitivity of the modeled mole fractions to changes in emissions.

2.3 Chemical transport model

The Model of Ozone and Related chemical Tracers (MOZARTv4.5) is a 3-dimensional chemical transport model (Emmons et al., 2010). MOZARTv4.5 was run offline to produce the reference run of modeled atmospheric mole fractions, using the emissions described in Sect. 2.2, and to estimate the sensitivities of the atmospheric mole fractions to emission perturbations. Meteorological data were provided from the National Centers for Environmental Prediction/National Center for Atmospheric Research (NCEP/NCAR) reanalysis (Kalnay et al., 1996). The NCEP/NCAR reanalysis for use in MOZARTv4.5 are available from 1990 to 2008 every 6 h at a horizontal resolution of 1.8° longitude by 1.8° latitude and with 28 vertical levels in sigma coordinates, from the surface to 3 hPa. MOZARTv4.5 interpolated the meteorological data to a resolution of 2.8° longitude by 2.8° latitude, which was the chosen horizontal resolution of the model runs. For years prior to 1990, NCEP/NCAR reanalysis data from 1990 were used

repeatedly; and for years after 2008, the 2008 meteorological data were repeated. The PFCs were treated as tracers and no chemistry was input into MOZART; this is a reasonable assumption given their lifetimes are on the order of thousands of years (Ravishankara et al., 1993). A zero initial condition field was assumed for all of the high molecular weight PFCs, with an initial year based on EDGARv4.2's first non-zero emissions of 1971 for C_4F_{10}, 1986 for C_5F_{12}, C_7F_{16} and C_8F_{18}, and 1980 for C_6F_{14}. The upwind cells of the observation stations were chosen in MOZARTv4.5, as the observations are assumed to be representative of background air (Rigby et al., 2010).

In order to estimate the sensitivities of the atmospheric mole fractions to changes in emission rates, MOZARTv4.5 was run with annual emissions increased by 10 % from the reference run for one year. In the subsequent year, the emissions were returned to those of the reference run. This provided an estimate of the sensitivities of mole fractions at the observation grid cells to annual emission changes. Due to the computational expense of running MOZARTv4.5, these sensitivities were only tracked in the model for two years, and then the values were estimated to decay exponentially, with a one year decay time, to a globally mixed background value.

2.4 Inverse method

To derive global emissions, we used an inverse method that included constraints by the atmospheric observations and an independent estimate of the annual growth in emissions (Rigby et al., 2011). Often a minimum variance Bayesian approach is taken for atmospheric measurement-based emission estimates while using an independent estimate of absolute emissions, also known as prior, as a constraint. However, if the prior emission information is largely biased, as is the case for C_4F_{10} and C_5F_{12}, a large uncertainty is often assumed on the prior. This results in the prior providing little information on the derived emissions if observations are available. Alternatively, if observations are not available for a certain year, then the derived emissions can exhibit unphysical fluctuations due to the biased prior constraining the emissions. The growth-based Bayesian inverse approach, which incorporates the growth rate of emissions as prior information instead of absolute emission rates, overcomes some of these potential biases (Rigby et al., 2011). This inverse method acts to minimize the residuals of the atmospheric observations from the modeled mole fractions and the growth rate in the derived emissions from an independent estimate of the emission growth rate. These two constraints are weighted by the inverse of their relative uncertainties in determining the optimal solution. Here, the observations were weighted by their observational error, as described in Sect. 2.1. The assumed independent growth rate was the annual average growth rate in emissions for each species from EDGARv4.2. EDGARv4.2 does not provide an uncertainty estimate and because of the underestimation in C_4F_{10} and C_5F_{12} in the EDGARv4.2 estimates, the error assumed on the growth rate for C_4F_{10} and C_5F_{12} was the annual mean growth rate in emissions for C_4F_{10}, C_5F_{12}, C_6F_{14} and C_7F_{16} from EDGARv4.2. For C_6F_{14}, the assumed error was the annual mean growth rate in emissions from 1980 to 2008 of C_6F_{14} from EDGARv4.2, and likewise for C_7F_{16} and C_8F_{18}. Due to the low temporal frequency of the observations, only globally averaged emissions were resolved.

The year of emission onset in EDGARv4.2 appears to be later than the observations suggest – as observations are non-zero in earlier years. Therefore, an initial condition was also solved for in the inversion. The initial condition was applied globally; as the first SH observation is 5 yr after the first NH observation, this should not have a large influence on the derived emissions. In addition, we included an estimate of the uncertainty in the use of repeated dynamics in the derived emission estimates using a Monte Carlo approach, where the inversion was repeated 1000 times with randomly varied sensitivities of the modeled mole fractions to perturbations in emissions. The distribution of varied sensitivities was estimated by running the model multiple times with meteorological data from different years and calculating the mole fraction sensitivities, while the emissions and initial conditions were held constant (Rigby et al., 2010). This error was found to be relatively small compared to the error propagated through the inversion, and was added in quadrature to give the final estimate of emission uncertainty. The uncertainty on the derived emissions was estimated from the diagonal elements of the error covariance matrix and is based on the relative weighting of the uncertainty associated with the observations as compared to the uncertainty associated with the assumed growth rate constraint on emissions (Rigby et al., 2011).

3 Radiative efficiencies of C_7F_{16} and C_8F_{18}

3.1 Infrared absorption cross-sections

Roehl et al. (1995) reported infrared absorption cross-sections and GWPs for CF_4, C_2F_6, C_3F_8, C_4F_{10}, C_5F_{12} and C_6F_{14} while Bravo et al. (2010), more recently, similarly for C_8F_{18}. In the present work, we measured infrared absorption spectra of C_7F_{16} and C_8F_{18} using Fourier Transform Infrared (FTIR) spectroscopy. To the best of our knowledge there are no previously published infrared absorption spectrum measurements for C_7F_{16} available.

The C_7F_{16} (≥ 98 %) and C_8F_{18} (≥ 99 %) samples were purchased from Synquest Laboratories. These samples were vacuum distilled to remove non-condensables prior to use. Various dilute gas mixtures of the samples in a Helium (He) bath gas were prepared manometrically in 12-l Pyrex bulbs for use in the infrared spectrum measurements. Absorption spectra were measured between 500 and 4000 cm^{-1} at a spectral resolution of 1 cm^{-1}. Spectra were obtained using

Table 2. Infrared Absorption Band Strengths for C_7F_{16} and C_8F_{18} at 296 K.

Perfluoroheptane [C_7F_{16}]		Perfluorooctane [C_8F_{18}]	
Spectral Range [cm^{-1}]	Band Strength [10^{-17} cm^2 mol^{-1} cm^{-1}]	Spectral Range [cm^{-1}]	Band Strength [10^{-17} cm^2 mol^{-1} cm^{-1}]
500-1075	8.10±0.30	500-1100	8.60±0.30
1075-1375	36.10±0.40	1100-1400	40.80±0.40

two different pathlength absorption cells: a single-pass 16 cm long cell and a low-volume multi-pass cell (750 cm^3, 485 cm optical pathlength). Infrared absorption band strengths (absorption cross-sections) were obtained using Beer's law with spectra recorded over a range of sample concentrations at various bath gas pressures. The infrared spectra of C_7F_{16} and C_8F_{18} were independent of bath gas pressure for pressures between 20 and 600 Torr (He bath gas). The sample concentrations in the infrared absorption cell were varied over the range (0.10–8.28) $\times 10^{15}$ mol cm^{-3} for C_7F_{16} and (0.05–7.08) $\times 10^{15}$ mol cm^{-3} for C_8F_{18}, where the sample concentrations were determined using absolute pressure measurements and the known mixing ratio.

Figure 3 shows the infrared absorption spectra of C_7F_{16} and C_8F_{18}. The C_7F_{16} and C_8F_{18} spectra show weak absorption between 500 and 1000 cm^{-1}, but strong absorption bands between 1000 and 1400 cm^{-1}, where the integrated absorption band strengths were determined to be $(3.61 \pm 0.04) \times 10^{-16}$ cm^2 mol^{-1} cm^{-1} for C_7F_{16} (1075–1375 cm^{-1}) and $(4.08 \pm 0.04) \times 10^{-16}$ cm^2 mol^{-1} cm^{-1} for C_8F_{18} (1100–1400 cm^{-1}), see Table 2. The quoted uncertainties are at the 2-σ (95 % confidence) level and include estimated systematic uncertainties. The infrared absorption spectra data of C_7F_{16} and C_8F_{18} are provided in the Supplement.

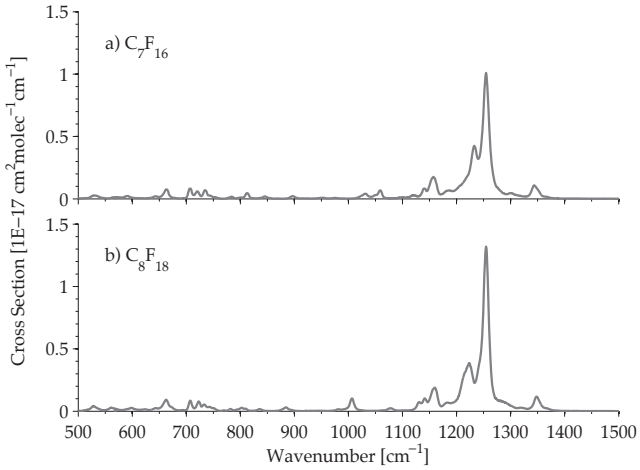

Fig. 3. Average absorption cross-section for **(a)** C_7F_{16} and **(b)** C_8F_{18} measured at 1 cm^{-1} resolution and 296 K. The spectra were measured over a range of 500–4000 cm^{-1}, although only the main spectral features are shown.

3.2 Radiative efficiencies

In order to estimate the relative change in radiative forcing per change in atmospheric concentrations, the radiative efficiencies were estimated for C_7F_{16} and C_8F_{18} using the spectra measured here and the method given by Pinnock et al. (1995). The radiative efficiency for C_7F_{16} and C_8F_{18} are 0.48 and 0.57 W m^{-2} ppb^{-1}, respectively, see Table 1. The radiative efficiency for C_8F_{18} is approximately equal to that of trifluoromethyl sulfur pentafluoride (SF_5CF_3), which is the highest of any measured atmospheric species (Forster et al., 2007).

The radiative efficiencies reported here are in reasonably good agreement, within 7 %, with those estimated by Bravo et al. (2010). The infrared measurements by Bravo et al. (2010) for C_8F_{18} were limited to the spectral range 700–1400 cm^{-1}. A radiative efficiency value, based on our measurements, of 0.53 W m^{-2} ppb^{-1} for C_8F_{18} can be obtained if a spectral range of 700–1400 cm^{-1} is used. Therefore we attribute the difference between the reported value from Bravo et al. (2010) and the value from this study for C_8F_{18} to the different spectral ranges of the measurements. The radiative efficiencies by Bravo et al. (2010), based on theoretical calculations and that include a larger spectral range 0–2500 cm^{-1}, are closer to our results for C_8F_{18}, with a difference of 3.6 %. Bravo et al. (2010) did not measure the infrared spectra of C_7F_{16} and provide a theoretical calculation of C_7F_{16}'s radiative efficiency at 0.45 W m^{-2} ppb^{-1}, which is in good agreement with the results from the present work.

3.3 Global warming potential

Global warming potentials (GWPs) provide a measure of the climate impact of emissions of a trace gas relative to a reference gas, usually chosen as carbon dioxide (CO_2) (Forster et al., 2007; United Nations Environment Programme, 1999). The radiative efficiencies, along with an estimate of the species' atmospheric lifetimes, allow for GWPs to be estimated. Following the standard method outlined by Forster et al. (2007), the GWPs were calculated for C_7F_{16} and C_8F_{18}. No lifetimes have been estimated for C_7F_{16} and C_8F_{18}. Ravishankara et al. (1993) determined that the major atmospheric removal pathway for the perfluoroalkanes, CF_4

through C_6F_{14}, was via photolysis by hydrogen Lyman-α radiation (121.6 nm) with a possible minor pathway due to reaction with O(^{1}D). Based on the work by Ravishankara et al. (1993), we assume that C_7F_{16} and C_8F_{18} will have similar lifetimes, on the order of thousands of years, and have chosen a lifetime of 3000 yr for the GWP calculations, which is close to the lifetime of C_6F_{14}. The GWPs for C_7F_{16} and C_8F_{18} are estimated to be 7930 and 8340 for a 100-yr time horizon with CO_2 as the reference gas, see Table 1. As the expected lifetimes of C_7F_{16} and C_8F_{18} are much longer than the chosen time horizons, these GWP calculations are relatively insensitive to the assumed lifetime. To confirm this, a sensitivity analysis to the assumed lifetime in the GWP estimate was done following Shine et al. (2005). A difference of 7.9 % and 1.1 % was found in the calculated 100-yr time horizon GWPs when using assumed lifetimes of 500 instead of 3000 yr or 10 000 instead of 3000 yr, respectively.

4 Results and discussion

The reference run of modeled mole fractions using the bottom-up estimates from EDGARv4.2 (see Sect. 2.2) in MOZARTv4.5 are presented in Fig. 1; the reference modeled mole fractions are lower than the atmospheric observations for the high molecular weight PFCs. In particular, the reference run produces modeled mole fractions that are 20 times and over a 1000 times too low for C_4F_{10} and C_5F_{12}, respectively. For C_5F_{12} this is due to the global annual emissions from EDGARv4.2 peaking at less than 0.1 t yr^{-1}, with the only emission source being use as refrigerants in Romania (ER-JRC/PBL, 2011). In contrast, the reference modeled mole fractions for C_6F_{14} are similar to the observations, although the reference run is somewhat lower in the mid-1990s, suggesting an underestimation of emissions during this period. For C_7F_{16} and C_8F_{18}, the reference run is about 50 % lower than atmospheric observations.

Using our inverse method, we provide new global emission estimates based on atmospheric observations. The derived emissions and their associated uncertainties are presented in Fig. 4 and Table 3. The derived emissions for C_4F_{10} and C_5F_{12} are relatively constant over the time period with an average emission rate and uncertainty of 196 ± 33 t yr^{-1} and 171 ± 42 t yr^{-1}, respectively. The C_4F_{10} and C_5F_{12} emissions exhibit the largest decline from 1999 to 2005. Comparison with the bottom-up estimates show that EDGARv4.2 emissions are 20 and 1000 times lower than the derived emissions for C_4F_{10} and C_5F_{12}, respectively, (with the 2008 EDGARv4.2 estimate at 9.6 kg yr^{-1} for C_5F_{12}, as compared to 67 ± 53 t yr^{-1} as derived in this study). Furthermore, the EDGARv4.2 emission temporal profile is drastically different than those derived from the observations, with emissions in EDGARv4.2 being relatively lower in the 1980s and then increasing with time.

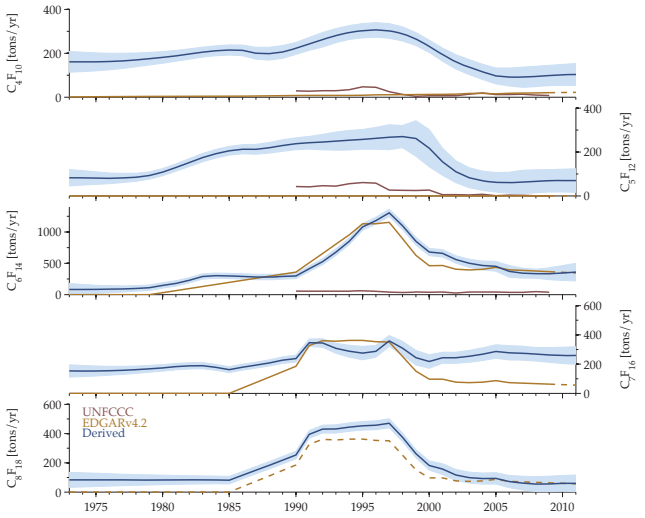

Fig. 4. The global annual emissions for C_4F_{10}, C_5F_{12}, C_6F_{14}, C_7F_{16} and C_8F_{18} derived in this study are shown as the solid blue line, and the associated 1-σ uncertainty in the emissions is represented as the light blue shading. The available bottom-up emissions data are also shown from EDGARv4.2 (solid yellow line) and UNFCCC (solid purple line). The interpolated data used in the reference run from EDGARv4.2 from 2009 to 2011 are shown as the dashed blue line, and the C_8F_{18} reference emissions are also shown as a dashed line, as no bottom-up estimates are available and C_7F_{16}'s emissions were used as a proxy.

In contrast, the derived emissions for C_6F_{14} agree fairly well with EDGARv4.2. The C_6F_{14} increase in emissions has a later onset, starting in the 1990s, than that of C_4F_{10} and C_5F_{12}, and has a similar emission profile as that of C_3F_8, shown in Mühle et al. (2010). Furthermore, the changes in the temporal profile in emissions coincides with the signing and coming into effect of the Montreal and Kyoto Protocols. Particularly, the C_6F_{14} emissions start to increase in the late 1980s, coinciding with the signing of the Montreal protocol, suggesting that C_6F_{14} was used as replacement compounds for ODSs. Of the PFCs studied here, C_6F_{14} has the largest emissions with a 1980 to 2010 average emission rate of 510 ± 62 t yr^{-1}.

The derived emissions for C_7F_{16} and C_8F_{18} are both higher than those of C_7F_{16} in EDGARv4.2. Interestingly while the other high molecular weight PFC emissions have decreased in the past 10 to 20 yr, the derived emissions for C_7F_{16} are relatively constant for the last ten years, with an average emission rate over the entire study period of 251 ± 37 t yr^{-1}. The average emission rate for C_8F_{18} is 195 ± 34 t yr^{-1}.

Our derived emissions for C_4F_{10} and C_5F_{12} agree fairly well with those presented by Laube et al. (2012). However, we see discrepancies for C_6F_{14} and C_7F_{16}. In particular, Laube et al. (2012) estimates lower emission rates from 1994 to 2001 than ours for C_6F_{14}. The C_6F_{14} observations from Laube et al. (2012) agree well with those presented in Ivy

Table 3. Annual mean global emission rates and uncertainties for C_4F_{10}, C_5F_{12}, C_6F_{14}, C_7F_{16} and C_8F_{18}.

Year	C_4F_{10} [t yr^{-1}]	C_5F_{12} [t yr^{-1}]	C_6F_{14} [t yr^{-1}]	C_7F_{16} [t yr^{-1}]	C_8F_{18} [t yr^{-1}]
1980	181 ± 27	108 ± 16	147 ± 44	174 ± 22	83 ± 32
1981	188 ± 25	129 ± 17	179 ± 43	183 ± 22	83 ± 30
1982	197 ± 23	152 ± 18	229 ± 43	188 ± 22	83 ± 29
1983	205 ± 23	174 ± 19	290 ± 43	189 ± 21	84 ± 27
1984	211 ± 23	192 ± 20	303 ± 42	178 ± 20	83 ± 26
1985	215 ± 23	206 ± 20	300 ± 42	162 ± 20	81 ± 26
1986	213 ± 24	213 ± 21	289 ± 42	179 ± 20	116 ± 25
1987	200 ± 27	212 ± 22	279 ± 43	193 ± 21	150 ± 25
1988	198 ± 29	219 ± 24	284 ± 43	208 ± 21	183 ± 25
1989	206 ± 29	229 ± 26	290 ± 43	227 ± 22	218 ± 25
1990	222 ± 27	238 ± 27	298 ± 43	238 ± 24	253 ± 26
1991	243 ± 30	242 ± 29	414 ± 45	346 ± 26	395 ± 26
1992	262 ± 33	245 ± 35	526 ± 49	345 ± 29	431 ± 27
1993	280 ± 32	249 ± 41	678 ± 52	308 ± 34	432 ± 28
1994	295 ± 32	254 ± 45	851 ± 53	288 ± 41	444 ± 29
1995	303 ± 33	258 ± 45	1080 ± 53	275 ± 46	453 ± 30
1996	307 ± 33	262 ± 50	1182 ± 55	287 ± 41	457 ± 30
1997	302 ± 34	267 ± 57	1305 ± 59	359 ± 37	471 ± 31
1998	288 ± 32	270 ± 50	1100 ± 61	309 ± 47	374 ± 29
1999	265 ± 29	261 ± 81	852 ± 61	244 ± 50	263 ± 28
2000	232 ± 28	218 ± 85	681 ± 58	218 ± 46	182 ± 32
2001	194 ± 30	155 ± 62	659 ± 58	244 ± 38	158 ± 37
2002	161 ± 33	110 ± 50	561 ± 60	243 ± 38	117 ± 38
2003	137 ± 34	83 ± 46	501 ± 65	254 ± 41	99 ± 38
2004	115 ± 35	69 ± 44	466 ± 71	268 ± 44	92 ± 38
2005	97 ± 36	62 ± 45	452 ± 78	286 ± 46	93 ± 39
2006	92 ± 41	60 ± 48	371 ± 94	278 ± 49	72 ± 42
2007	91 ± 47	64 ± 53	343 ± 80	274 ± 49	62 ± 47
2008	95 ± 47	67 ± 53	334 ± 72	268 ± 46	55 ± 52
2009	99 ± 46	69 ± 51	333 ± 95	262 ± 51	56 ± 53
2010	102 ± 48	70 ± 52	345 ± 118	260 ± 56	60 ± 53

et al. (2012) in the early 1980s and 1990s; however after this time period the observations by Laube et al. (2012) are lower than those in Ivy et al. (2012). This is most likely due to a calibration scale difference, with that of Laube et al. (2012) estimating lower mole fractions than Ivy et al. (2012), and possible nonlinearities in the early archive measurements. We see a general underestimation of C_7F_{16} emissions by Laube et al. (2012) compared with those estimated in this study. This is most likely due to the lower calibration scale by Laube et al. (2012) as compared with Ivy et al. (2012). Laube et al. (2012) used an 85 % *n*-isomer of C_7F_{16} for their calibration scale and subsequently estimate an atmospheric mole fraction in 2010 that is 13 % lower. Laube et al. (2012) did not present atmospheric measurements or emission estimates for C_8F_{18}. Furthermore as no bottom-up estimates are available either, the C_8F_{18} emissions derived in this study are the first published estimates.

Overall the UNFCCC reported inventories are five to ten times lower than the emissions derived based on the observations for C_4F_{10}, C_5F_{12} and C_6F_{14}. In general, the UNFCCC emission inventories could be considered a lower bounds on

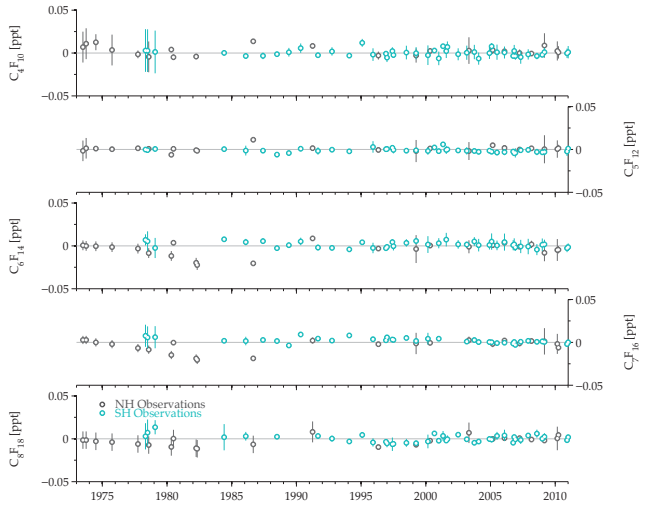

Fig. 5. The mole fraction residuals, taken as the observations minus final modeled mole fractions (Northern Hemisphere – grey and Southern Hemisphere – light blue). The vertical lines represent the uncertainty associated with each observation. A zero line is also plotted for reference.

global emissions as they do not include some major greenhouse gas emitters. Both C_7F_{16} and C_8F_{18} are not reported to UNFCCC; however based on our results, their emissions are larger than those of C_4F_{10} and C_5F_{12} and should be considered in future inventories.

MOZARTv4.5 was run using the derived emissions and produced modeled mole fractions that were much closer to the observations (as required in the inversion), see Fig. 1. Figure 5 shows the residuals of the final runs (take as the observed mole fractions minus the final modeled mole fractions) using the derived emissions. Most of the residuals are within the estimated observational error and no significant trends in the residuals are found, confirming that the derived emissions represent an improved estimate.

Using the 100-yr time horizon GWPs, we provide an update to the total annual global PFC emissions in CO_2 equivalents (Fig. 6). CF_4, C_2F_6 and c−C_4F_8 contribute the most to the radiative forcing of the PFC emissions. However, we find that the high molecular weight PFCs contribute significantly to the total PFC budget, with the C_6F_{14} emissions being comparable to those of C_3F_8. Previous estimates of the radiative forcing of PFC emissions in 2009, which only included CF_4, C_2F_6, C_3F_8 and c−C_4F_8, are 111 600 Gg CO_2 equivalents in 2009 (Mühle et al., 2010; Oram et al., 2012); inclusion of the high molecular weight PFCs increases this number by 6 % to 118 700 Gg CO_2-eq.

The high molecular weight PFC emissions from 1973 to 2010 have contributed 400 000 Gg of CO_2 equivalents to global radiative forcing. Moreover, the peak in cumulative emissions of the high molecular weight PFCs was in 1997, which coincides with the signing of the Kyoto Protocol, at 24 000 Gg of CO_2 equivalents. Subsequently, emissions have

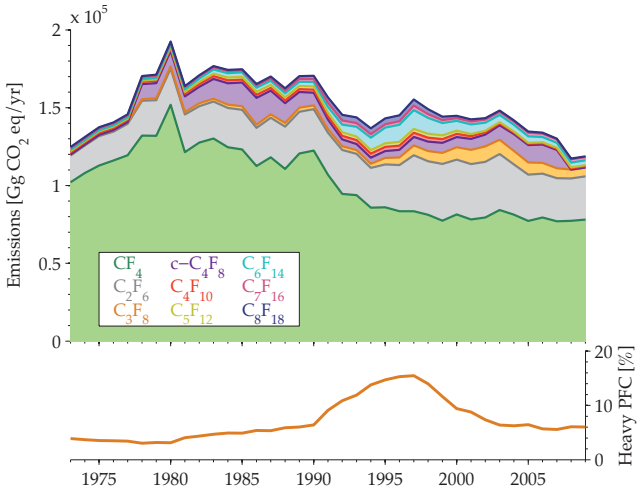

Fig. 6. Global annual PFC emissions in CO_2 equivalents, using GWPs with a 100-yr time horizon, from 1973 to 2009. The CF_4, C_2F_6 and C_3F_8 emissions are from Mühle et al. (2010) and the $c-C_4F_8$ emissions are from Oram et al. (2012). The bottom panel shows the relative percentage the high molecular weight PFCs studied here contribute to the new global total of PFC emissions in CO_2 equivalents.

declined by a factor of three to 7300 Gg of CO_2 equivalents in 2010. This 2010 cumulative emission rate is comparable to: 0.02 % of the total CO_2 emissions, 0.81 % of the total hydrofluorocarbon emissions and 1.07 % of the chlorofluorocarbon emissions projected for 2010 (Velders et al., 2009). The largest contribution of the high molecular weight PFCs to the global PFC emission budget was also in 1997, when they contributed 15.4 % of the total emissions. Since 1997, the relative contribution of the high molecular weight PFCs to global emissions has decreased, most likely due to their replacement with low GWP alternatives (Office of Air and Radiation and Office of Atmospheric Programs, 2006).

5 Conclusions

In this study, global emission estimates from 1973 to 2010 have been presented for C_4F_{10}, C_5F_{12}, C_6F_{14}, C_7F_{16} and C_8F_{18} using new atmospheric observations and an independent growth constraint on emissions. The temporal profile of emissions of the high molecular weight PFCs, shows an onset of increased emissions in the late 1980s, coinciding with the signing of the Montreal Protocol, and a decline in emissions starting from 1997, coinciding with the signing of the Kyoto Protocol. We find a significant underestimation in emissions by EDGARv4.2 for C_4F_{10} and C_5F_{12}, further illustrating the benefit of atmospheric-observations based emission estimates in verifying bottom-up emission estimates. Additionally, the reported inventories to UNFCCC by Annex 1 countries that have ratified the Kyoto Protocol are generally five to ten times lower than the derived emission rates for C_4F_{10}, C_5F_{12} and C_6F_{14}. However the derived emissions are global, therefore this discrepancy cannot be attributed to individual countries. These large discrepancies between the derived and bottom-up estimates highlight the need for more transparent and accurate reporting of emissions. Interestingly, the UNFCCC reported inventories show similar temporal trends as the derived emissions, suggesting the UNFCCC methodology may be a good platform for emissions reporting.

Using the newly derived GWPs for C_7F_{16} and C_8F_{18}, new estimates of the total radiative impact of all PFC emissions are an average 7 % higher than previously reported for 1973 to 2009. The high molecular weight PFCs contributed most significantly to the global PFC emissions, up to 16 %, in the 1990s, indicating a previous underestimation of the total radiative forcing from PFC emissions. While emissions have declined in the past 10 yr, because of their long lifetimes, PFCs are considered to have a nearly permanent effect on the Earth's radiative budget on human timescales. Therefore, continued monitoring of atmospheric abundances is necessary to detect trends in emissions of these potent greenhouse gases.

Supplementary material related to this article is available online at: http://www.atmos-chem-phys.net/12/7635/2012/acp-12-7635-2012-supplement.zip.

Acknowledgements. This research is supported by the NASA Upper Atmospheric Research Program in the US with grants NNX11AF17G to MIT and a consortium of 40 industrial and foundation sponsors of the MIT Joint Program on the Science and Policy of Global Change (see http://globalchange.mit.edu/sponsors/current.html). The work at NOAA was supported by NOAA's Climate Goal. We would like to thank Stacy Walters and Louisa Emmons for their help and advice on the use of the MOZART model. We also thank the two anonymous referees for their helpful comments.

Edited by: R. Harley

References

3M Electronics Markets Materials Division: Performance Fluid PF-5060, 3M, St. Paul, MN, USA, 2003.

Air and Radiation Global Programs Division: Substitutes in Non-Aerosol Solvent Cleaning Under SNAP as of September 28, 2006, US EPA Report, United States Environmental Protection Agency, Washington DC, USA, 2006.

Bravo, I., Aranda, A., Hurley, M. D., Marston, G., Nutt, D. R., Shine, K. P., Smith, K., and Wallington, T. J.: Infrared absorption spectra, radiative efficiencies, and global warming potentials of perfluorocarbons: comparison between experiment and theory, J. Geophys. Res., 115, D24317, doi:10.1029/2010JD014771, 2010.

Chen, Y.-H. and Prinn, R. G.: Estimation of atmospheric methane emissions between 1996 and 2001 using a three-dimensional global chemical transport model, J. Geophys. Res., 111, 1–25, D10307, doi:10.1029/2005JD006058, 2006.

Deeds, D. A., Vollmer, M. K., Kulongoski, J. T., Miller, B. R., Mühle, J., Harth, C. M., Izbicki, J. A., Hilton, D. R., and Weiss, R. F.: Evidence for crustal degassing of CF_4 and SF_6 in Mojave Desert groundwaters, Geochim. Cosmochim. Ac., 72, 999–1013, doi:10.1016/j.gca.2007.11.027, 2008.

Emmons, L. K., Walters, S., Hess, P. G., Lamarque, J.-F., Pfister, G. G., Fillmore, D., Granier, C., Guenther, A., Kinnison, D., Laepple, T., Orlando, J., Tie, X., Tyndall, G., Wiedinmyer, C., Baughcum, S. L., and Kloster, S.: Description and evaluation of the Model for Ozone and Related chemical Tracers, version 4 (MOZART-4), Geosci. Model Dev., 3, 43–67, doi:10.5194/gmd-3-43-2010, 2010.

European Commission, Joint Research Centre (JRC)/Netherlands Environmental Assessment Agency (PBL): Emission Database for Global Atmospheric Research (EDGAR), Release 4.2, available at: http://edgar.jrc.ec.europa.eu, (last access: 15 December 2011), 2011.

Fenhann, J.: HFC, PFC and SF_6 emission scenarios: recent developments in IPCC special report on emission scenarios, in: Proceedings of Joint IPCC/TEAP expert meeting on options for limitation of emissions of HFCs and PFCs, The Netherlands Ministry of the Environment and United States Environmental Protection Agency, Petten, Netherlands, 15–33, 1999.

Forster, P., Ramaswamy, V., Artaxo, P., Berntsen, T., Betts, R., Fahey, D. W., Haywood, J., Lean, J., Lowe, D. C., Myhre, G., Nganga, J., Prinn, R., Raga, G., Schulz, M., and Van Dorland, R.: Changes in atmospheric constituents and in radiative forcing, in: Climate Change 2007: The Physical Science Basis. Contribution of Working Group 1 to the Fourth Assessment Report of the Intergovernmental Panel on Climate Change, edited by: Solomon, S., Qin, D., Manning, M., Chen, Z., Marquis, M., Averyt, K. B., Tignor, K. B., and Miller, H. L., Cambridge Univ. Press, Cambridge, UK and New York, NY, USA, 2007.

Forte Jr., R., McCulloch, A., and Midgley, P.: Emissions of substitutes for ozone-depleting substances, in: Good Practice Guidance and Uncertainty Management in National Greenhouse Gas Inventories, IPCC National Greenhouse Gas Inventories Programme, Kanagawa, Japan, 257–270, 2003.

Harnisch, J., Borchers, R., Fabian, P., Gäggeler, H. W., and Schotterer, U.: Effect of natural tetrafluoromethane, Nature, 384, 32, doi:10.1038/384032a0, 1996a.

Harnisch, J., Borchers, R., Fabian, P., and Maiss, M.: Tropospheric trends for CF_4 and C_2F_6 since 1982 derived from SF_6 dated stratospheric air, Geophys. Res. Lett., 23, 1099–1102, doi:10.1029/96GL01198, 1996b.

Harvey, R.: Estimates of US Emissions of High-Global Warming Potential Gases and the Costs of Reductions, US Environmental Protection Agency, Washington, DC, USA, 2000.

International Aluminium Institute: Results of the 2010 Anode Effect Survey: Report on the Aluminum Industry's Global Perfluorocarbon Gases Emissions Reduction Programme, International Aluminium Institute, London, UK, 2011.

Ivy, D. J., Arnold, T., Harth, C. M., Steele, L. P., Mühle, J., Rigby, M., Salameh, P. K., Leist, M., Krummel, P. B., Fraser, P. J., Weiss, R. F., and Prinn, R. G.: Atmospheric histories and growth trends of C_4F_{10}, C_5F_{12}, C_6F_{14}, C_7F_{16} and C_8F_{18}, Atmos. Chem. Phys., 12, 4313–4325, doi:10.5194/acp-12-4313-2012, 2012.

Kalnay, E., Kanamitsu, M., Kistler, R., Collins, W., Deaven, D., Gandin, L., Iredell, M., Saha, S., White, G., Woollen, J., Zhu, Y., Chelliah, M., Ebisuzaki, W., Higgins, W., Janowiak, J., Mo, K. C., Ropelewski, C., Wang, J., Leetmaa, A., Reynolds, R., Jenne, R., and Joseph, D.: The NCEP/NCAR 40-yr Reanalysis Project, B. Am. Meteorol. Soc., 77, 437–471, doi:10.1175/1520-0477(1996)077, 1996.

Kopylov, S. N.: The influence of oxidation of HFC's and FC's on their fire extinguishing and explosion preventing characteristics, in: Halon Alternatives Technical Working Conference, edited by: Gann, R. G. and Reneke, P. A., Proceedings HOTWC, Albuquerque, NM, USA, 342–349, 2002.

Laube, J. C., Hogan, C., Newland, M. J., Mani, F. S., Fraser, P. J., Brenninkmeijer, C. A. M., Martinerie, P., Oram, D. E., Röckmann, T., Schwander, J., Witrant, E., Mills, G. P., Reeves, C. E., and Sturges, W. T.: Distributions, long term trends and emissions of four perfluorocarbons in remote parts of the atmosphere and firn air, Atmos. Chem. Phys., 12, 4081–4090, doi:10.5194/acp-12-4081-2012, 2012.

Mühle, J., Ganesan, A. L., Miller, B. R., Salameh, P. K., Harth, C. M., Greally, B. R., Rigby, M., Porter, L. W., Steele, L. P., Trudinger, C. M., Krummel, P. B., O'Doherty, S., Fraser, P. J., Simmonds, P. G., Prinn, R. G., and Weiss, R. F.: Perfluorocarbons in the global atmosphere: tetrafluoromethane, hexafluoroethane, and octafluoropropane, Atmos. Chem. Phys., 10, 5145–5164, doi:10.5194/acp-10-5145-2010, 2010.

Office of Air and Radiation and Office of Atmospheric Programs, Climate Change Division: Uses and Emissions of Liquid PFC Heat Transfer Fluids from the Electronics Sector, in: US EPA Report EPA-430-R-06-901, United States Environmental Protection Agency, Washington DC, USA, 2006.

Oram, D. E., Mani, F. S., Laube, J. C., Newland, M. J., Reeves, C. E., Sturges, W. T., Penkett, S. A., Brenninkmeijer, C. A. M., Röckmann, T., and Fraser, P. J.: Long-term tropospheric trend of octafluorocyclobutane (c-C_4F_8 or PFC-318), Atmos. Chem. Phys., 12, 261–269, doi:10.5194/acp-12-261-2012, 2012.

Pinnock, S., Hurley, M. D., Shine, K. P., Wallington, T. J., and Smyth, T. J.: Radiative forcing of climate by hydrochlorofluorocarbons and hydrofluorocarbons, J. Geophys. Res., 100, 23227–23238, doi:10.1029/95JD02323, 1995.

Prinn, R. G.: Measurement equation for trace chemicals in fluids and solution of its inverse, in: Inverse Methods in Global Biogeochemical Cycles, Geophys. Monogr. Ser., vol 114, edited by: Kasibhatla, P., AGU, Washington DC, USA, 3–18, doi:10.1029/GM114p0003, 2000.

Ravishankara, A. R., Solomon, S., Turnipseed, A. A., and Warren, R. F.: Atmospheric lifetimes of long-lived halogenated species, Science, 259, 194–199, doi:10.1126/science.259.5092.194, 1993.

Rigby, M., Mühle, J., Miller, B. R., Prinn, R. G., Krummel, P. B., Steele, L. P., Fraser, P. J., Salameh, P. K., Harth, C. M., Weiss, R. F., Greally, B. R., O'Doherty, S., Simmonds, P. G., Vollmer, M. K., Reimann, S., Kim, J., Kim, K.-R., Wang, H. J., Olivier, J. G. J., Dlugokencky, E. J., Dutton, G. S., Hall, B. D., and Elkins, J. W.: History of atmospheric SF_6 from 1973 to

2008, Atmos. Chem. Phys., 10, 10305–10320, doi:10.5194/acp-10-10305-2010, 2010.

Rigby, M., Ganesan, A. L., and Prinn, R. G.: Deriving emissions time series from spare atmospheric mole fractions, J. Geophys. Res., 116, 1–7, D08306, doi:10.1029/2010JD015401, 2011.

Roehl, C. M., Boglu, D., Brühl, C., and Moortgat, G. K.: Infrared band intensities and global warming potentials of CF_4, C_2F_6, C_3F_8, C_4F_{10}, C_5F_{12}, and C_6F_{14}, Geophys. Res. Lett., 22, 815–818, doi:10.1029/95GL00488, 1995.

Semiconductor Industry Association: Semiconductor Industry Association Announces PFC Reduction and Climate Partnership with US EPA, Semiconductor Industry Association Press Release, Washington DC, USA, 2001.

Schwaab, K., Dettling, F., Bernhardt, D., Elsner, C., Sartorius, R., Reimann, K., Remus, R., and Plehn, W.: Fluorinated Greenhouse Gases in Products and Processes: an Evaluation of Technical Measures to Reduce Greenhouse Gas Emissions, German Federal Environmental Agency, Dessau, Germany, 2005.

Shine, K. P., Gohar, L. K., Hurley, M. D., Marston, G., Martin, D., Simmonds, P. G., Wallington, T. J., and Watkins, M.: Perfluorodecalin: global warming potential and first detection in the atmosphere, Atmos. Environ., 39, 1759–1763, doi:10.1016/j.atmosenv.2005.01.001, 2005.

Tsai, W.: Environmental hazards and health risk of common liquid perfluoro-n-alkanes, potent greenhouse gases, Environ. Int., 35, 418–424, doi:10.1016/j.envint.2008.08.009, 2009.

Tuma, P. and Tousignant, L.: Reducing emissions of PFC heat transfer fluids, presented at SEMI Technical Symposium, 3M Specialty Materials, San Francisco, CA, 16 July 2001, 1–8, 2001.

United National Framework Convention on Climate Change Secretariat: National greenhouse gas inventory data for the period 1990–2009, United Nations Office at Geneva, Geneva, Switzerland, 2011.

United Nations Environment Programme: The implications to the Montreal Protocol of the inclusion of HFCs and PFCs in the Kyoto Protocol, in: Technology and Economic Assessment Panel Report of the HFC and PFC Task Force, Ozone Secretariat, United Nations Environment Programme, Nairobi, Kenya, 1–86, 1999.

World Semiconductor Council: Semiconductor manufacturers reduce PFC emissions, World Semiconductor Council Press Release, Kyoto, Japan, 2005.

Velders, G. J. M., Fahey, D. M., Daniel, J. S., McFarland, M., Andersen, S. O.: The large contribution of projected HFC emissions to future climate forcing, PNAS, 106, 10949–10954, doi:10.1073/pnas.0902817106, 2009.

MIT JOINT PROGRAM ON THE SCIENCE AND POLICY OF GLOBAL CHANGE

REPRINT SERIES Recent Issues

Joint Program Reprints are available free of charge (limited quantities). To order: please use contact information on inside of front cover.

2012-32 The role of China in mitigating climate change, Paltsev, S., J. Morris, Y. Cai, V. Karplus and H.D. Jacoby, *Energy Economics*, 34(S3): S444–S450 (2012)

2012-33 Valuing climate impacts in integrated assessment models: the MIT IGSM, John Reilly, Sergey Paltsev, Ken Strzepek, Noelle E. Selin, Yongxia Cai, Kyung-Min Nam, Erwan Monier, Stephanie Dutkiewicz, Jeffery Scott, Mort Webster and Andrei Sokolov, *Climatic Change*, online first, doi:10.1007/s10584-012-0635-x (2012)

2012-34 From "Green Growth" to sound policies: An overview, Schmalensee, Richard, *Energy Economics*, 34: S–S6 (2012)

2012-35 Shale gas production: potential versus actual greenhouse gas emissions, O'Sullivan, F. and S. Paltsev, *Environmental Research Letters*, 7(4): 044030 (2012)

2012-36 Atmospheric histories and growth trends of C_4F_{10}, C_5F_{12}, C_6F_{14}, C_7F_{16}, C_8F_{18}, Ivy, D.J., T. Arnold, C.M. Harth, L.P. Steele, J. Mühle, M. Rigby, P.K. Salameh, M. Leist, P.B. Krummel, P.J. Fraser, R.F. Weiss and R.G. Prinn, *Atmospheric Chemistry and Physics*, 12: 4313–4325 (2012)

2012-37 Global emission estimates and radiative impact of C_4F_{10}, C_5F_{12}, C_6F_{14}, C_7F_{16}, C_8F_{18}, Ivy, D.J., M. Rigby, M. Baasandorj, J.B. Burkholder and R.J. Prinn, *Atmospheric Chemistry and Physics*, 12: 7635–7645 (2012)

2013-1 The Impact of Climate Policy on US Aviation, Winchester, Niven, Christoph Wollersheim, Regina Clewlow, Nicholas C. Jost, Sergey Paltsev, John M. Reilly and Ian A. Waitz, *Journal of Transport Economics and Policy*, 47(1): 1–15 (2013)

2013-2 Impact of anthropogenic absorbing aerosols on clouds and precipitation: A review of recent progresses, Wang, Chien, *Atmoshperic Research*, 122: 237–249 (2013)

2013-3 Applying engineering and fleet detail to represent passenger vehicle transport in a computable general equilibrium model, Karplus, Valerie, Sergey Paltsev, Mustafa Babiker and John M. Reilly, *Economic Modelling,* 30: 295–305 (2013)

2013-4 Should a vehicle fuel economy standard be combined with an economy-wide greenhouse gas emissions constraint? Implications for energy and climate policy in the United States, Karplus, Valerie, Sergey Paltsev, Mustafa Babiker and John M. Reilly, *Energy Economics*, 36: 322–333 (2013)

2013-5 Climate impacts of a large-scale biofuels expansion, Hallgren, W., C.A. Schlosser, E. Monier, D. Kicklighter, A. Sokolov and J. Melillo, *Geophysical Research Letters*, 40(8): 1624–1630 (2013)

2013-6 Non-nuclear, low-carbon, or both? The case of Taiwan, Chen, Y.-H.H., *Energy Economics*, 39: 53–65 (2013)

2013-7 The Cost of Adapting to Climate Change in Ethiopia: Sector-Wise and Macro-Economic Estimates, Robinson, S., K. Strzepek and Raffaello Cervigni, *IFPRI ESSP WP 53* (2013)

2013-8 Historical and Idealized climate model experiments: an intercomparison of Earth system models of intermediate complexity, Eby, M., A.J. Weaver, K. Alexander, K. Zickfield, A. Abe-Ouchi, A.A. Cimatoribus, E. Crespin, S.S. Drijfhout, N.R. Edwards, A.V. Eliseev, G. Feulner, T. Fichefet, C.E. Forest, H. Goosse, P.B. Holden, F. Joos, M. Kawamiya, D. Kicklighter, H. Kiernert, M. Matsumoto, I.I. Mokov, E. Monier, S.M. Olsen, J.O.P. Pedersen, M. Perrette, G. Phillpon-Berthier, A. Ridgwell, A Schlosser, T. Schneider von Deimling, G. Shaffer, R.S. Smith, R. Spahni, A.P. Sokolov, M. Steinacher, K. Tachiiri, K. Tokos, M. Yoshimori, N Zeng and F. Zhao, *Clim. Past*, 9:1111–1140 (2013)

2013-9 Correction to "Sensitivity of distributions of climate system properties to the surface temperature data set", and Sensitivity of distributions of climate system properties to the surface temperature data set, Libardoni, A.G. and C.E. Forest, *Geophysical Research Letters*, 40(10): 2309–2311 (2013), and 38(22): 1–6 (2011)

2013-10 Permafrost degradation and methane: low risk of biogeochemical climate-warming feedback, Gao, Xiang, C. Adam Schlosser, Andrei Sokolov, Katey Walter Anthony, Qianlai Zhuang and David Kicklighter, *Environmental Research Letters*, 8(3): 035014 (2013)

For a complete list of titles see:
http://globalchange.mit.edu/research/publications/reprints

MIT Joint Program on
The Science and Policy of Global Change
Massachusetts Institute of Technology
77 Massachusetts Avenue, E19-411
Cambridge, MA 02139
USA